Published in final edited form as:
Acta Biomater. 2010 February ; 6(2): . doi:10.1016/j.actbio.2009.08.043.

Bioactive Polymer Grafting onto Titanium Alloy Surfaces for Improved Osteointegration

Alexandra Michiardi[1], **Gérard Hélary**[2], **Phuong-Cac Thi Nguyen**[3], **Lara J. Gamble**[3], **Fani Anagnostou**[4], **David G. Castner**[3], and **Véronique Migonney**[2]

[1]Institute of Bioengineering of Catalonia (IBEC), Barcelona, Spain

[2]Laboratory of Biomaterials and Specialty Polymers (LBPS/CSPBAT – FRE CNRS 3043), Institut Galilée, Université Paris 13, 93430 Villetaneuse, France

[3]National ESCA and Surface Analysis Center for Biomedical Problems, Departments of Bioengineering and Chemical Engineering, Box 351750, University of Washington, Seattle, WA 98195-1750 USA

[4]Bioingéniérie et Biomécanique Ostéoarticulaire, (UMR CNRS 7052), Université Paris 7, 10 avenue de Verdun, 75010 Paris, France

Abstract

Bioactive polymers bearing sulfonate (styrene sodium sulfonate, NaSS) and carboxylate (methylacrylic acid, MA) groups were grafted onto Ti6Al4V alloy surfaces by a two-step procedure. The Ti alloy surfaces were first chemically oxidized in a piranha solution and then directly subjected to radical polymerization at 70°C in absence of oxygen. The grafted surfaces were characterized by X-ray photoelectron spectroscopy (XPS), time-of-flight secondary ion mass spectrometry (ToF-SIMS) and the Toluidin blue colorimetric method. Toluidin blue results showed 1 to 5 μg/cm^2 of polymer was grafted onto the oxidized Ti surfaces. Grafting resulted in a decrease in the XPS Ti and O signals from the underlying Ti substrate and a corresponding increase in the XPS C and S signals from the polymer layer. The ToF-SIMS intensities of the S^- and SO^- ions correlated linearly with the XPS atomic percent S concentrations and the ToF-SIMS intensity of the $TiO_3H_2^-$ ion correlated linearly with the XPS atomic percent Ti concentration. Thus, the ToF-SIMS S^-, SO^- and $TiO_3H_2^-$ intensities can be used to quantify composition and amount of grafted polymer. ToF-SIMS also detected ions that were more characteristic of the polymer molecular structure ($C_6H_4SO_3^-$ and $C_8H_7SO_3^-$ from NaSS, $C_4H_5O_2^-$ from MA), but the intensity of these peaks depended on the polymer thickness and composition. An *in vitro* cell culture test was carried out with human osteoblast-like cells to assess the influence of the grafted polymers on cell response. Cell adhesion after 30 min of incubation showed significant differences between the grafted and un-grafted surfaces. The NaSS grafted surfaces showed the highest degree of cell adhesion while the MA-NaSS grafted surfaces showed the lowest degree of cell adhesion. After 4 weeks *in vivo* in rabbit femoral bones bone was observed to be in direct contact with all implants. The percent of mineralized tissue around the implants was similar for NaSS grafted and non-grafted implants (59 and 57%). The MA-NaSS grafted implant exhibited a lower amount of mineralized tissue (47%).

Keywords

Titanium Alloy; Bioactive Polymers; Osteointegration; ToF-SIMS; XPS

Introduction

Ti with 6% Al and 4% V (Ti6Al4V) is presently used in orthopaedic applications due to a combination of good mechanical properties such as fatigue and corrosion resistance, low density, relatively low elastic modulus and chemical inertness of the oxide layer 1, 2. However, long-term success of Ti6Al4V implants and the completeness of their osteointegration still need to be addressed 3–5. To promote osteointegration, numerous strategies have been developed to create a bond between the implant and the living host tissue. The success of these strategies is strongly affected by the chemical and physical properties of the implant surface. A common strategy is to coat the implant material with a layer of hydroxyapatite (HAP), the mineral phase of bone, either via direct deposition of HAP or by a process that will form HAP. The apatite layer is a bioactive material which allows direct bonding of the implant with bone and hence forms a stronger mechanical anchorage of the implant to bone. Among the direct deposition methods, plasma spray (6) and sol-gel methods (7) have been widely employed. Other techniques such as laser coating (8) or high frequency induction heat gradient methods (9) have also been recently developed. However, the main disadvantages of these techniques are the weak adhesion between the coating and the substrate (10;11) and the *in vivo* dissolution of the apatite phase that can lead to the failure of the implant (12). A successful indirect method to make the implant surface bioactive has been developed by Kokubo and co-workers (13;14). It consists of a NaOH chemical treatment followed by a thermal treatment to create a specific surface chemical structure that once in contact with a biological fluid will lead to the deposition of an apatite layer onto the implant surface. Despite the efficiency of this process in several *in vitro* and *in vivo* studies, mainly using pure titanium substrates, it has yet to see wide-spread commercial implementation at the industrial-scale.

A variety of other methods that physically or chemically modify the material surface can be found in the literature, including ion implantation (15), laser surface treatment (16,17) and thermal treatment with or without shot blasting (18;19).

However, the existing surface treatment methods do not provide ideal bonding strength of the coating and the desired long-term implantation performance, so some improvement of these methods is still needed (20).

Recently some new techniques to functionalize biomaterial surfaces have been developed, especially for titanium (21–22). These provide promising approaches for tailoring biomaterial surface properties. Surface functionalization consists of tethering specific chemical groups with covalent bonds onto the surface of the material to elicit the desired biological response from the host. Depending on the clinical application, different chemical groups can be selected for grafting to the surface. Silanization of titanium surfaces has already been studied and its success greatly depends on pre-treatment steps such as the cleaning and oxidation of Ti (23). Silanization typically requires a second step to graft a bioactive chemical group onto the silanized surface. A direct grafting method of Ti with phosphonic acid groups (24) has given promising *in vitro* results, showing a higher production of collagen type I from osteoblasts cultured on the grafted surfaces compared to the same cells cultured on bare titanium surfaces (25).

To our knowledge, there are no published reports on grafting bioactive chemical groups onto the surface of Ti6Al4V alloys. We have previously shown that polymers bearing appropriate chemical functionalities such as sulfonate and carboxylate groups, when grafted onto surfaces, can modulate the cell attachment, spreading and activity of the materials. [26, 27] Previous studies have shown that grafting of styrene sodium sulfonate (NaSS) onto pure Ti surfaces results in enhanced osteoblast functionality. [22]

The aim of the current study was to graft polymers bearing sulfonate (NaSS) and carboxylate (methacrylic acid, MA) groups onto Ti6Al4V surfaces as a new method for improving the anchorage of hip prostheses into bone. Characterization of the surface functionalized was done using x-ray photoelectron spectroscopy (XPS), time-of-flight secondary ion mass spectrometry (ToF-SIMS) and the Toluidin blue colorimetric method. In vitro and in vivo biological evaluations of the grafted surfaces were also performed.

Materials and methods

Materials

Grafting of polymers was conducted on disks (diameter 13 mm) or cylinders (diameter 5 mm and length 12 mm) of Ti6Al4V alloy with the following bulk chemical composition: titanium 88.2%; Al 6.7%, V 4.5%; Fe 0.3%; organic contaminants 0.3%. These samples were furnished by CERAVER Company (France) and their surfaces polished with a series of SiC papers. The grit of the SiC paper used in the final polishing step was 1200.

The monomers used in the surface grafting experiments were NaSS (Fluka) and MA (Sigma-Aldrich). NaSS was purified by recrystallization in a mixture of water/ethanol (10/90 v/v) and MA was purified by distillation at 50°C under vacuum. After purification both were stored at 4°C before use.

Grafting procedure

Ti6Al4V disks or cylinders were cleaned by successive 10 min. ultrasound treatments in a bath of acetone followed a bath of distilled water. After drying, samples were oxidized for 1 or 3 min in a solution containing the same volume of pure H_2SO_4 and H_2O_2 (30%). The oxidation process was performed in a hermetic container with an oxygen-free environment. After oxidation samples were rinsed thoroughly in ultrapure water and then placed directly into a mechanically stirred solution of monomers: 0.7 $mol.l^{-1}$ NaSS or 2 $mol.l^{-1}$ MA:NaSS 80:20 (mol/mol). Radical polymerization was allowed to take place at 70°C for 15 hours under an oxygen-free atmosphere (22). Finally, samples were rinsed thoroughly in ultrapure water and dried. Samples were referenced as Ti_{alloy}, Ti_{NaSS} and $Ti_{MA/NaSS}$ for Ti6Al4V unmodified, grafted with polyNaSS and grafted with polyMA-NaSS respectively.

Surface characterization

Toluidin blue colorimetric method—Ti_{NaSS} and $Ti_{MA/NaSS}$ samples were immersed in a toluidine blue solution at 30°C for 6 hours to allow complexation of toluidine blue with the surface grafted polymers. [28] It is assumed that one mole of toluidine blue forms a complex with one mole of carboxylate groups or one mole of sulfonate groups. [29] Noncomplexed TB molecules were removed by gentle rinsing of the sample with a NaOH aqueous solution. Decomplexation of the toluidin blue was done by soaking the samples in 5 ml of an acetic acid solution (50 vol.% in water) for 24 h. Concentration of decomplexed toluidin blue was measured by visible spectroscopy at 633 nm using a Perkin Elmer lambda 25 spectrometer. Ungrafted Ti6Al4V samples were used as controls and were found not to react with the toluidine blue solution.

X-ray Photoelectron spectroscopy (XPS)—XPS data was acquired with a Surface Science Instruments S-probe spectrometer. This instrument has a monochromatized Al Kα X-ray source, hemispherical analyzer, multichannel detector and low-energy electron flood gun for charge neutralization. The X-ray spot size used for these experiments was approximately 800 μm × 800 μm. Pressure in the analytical chamber during spectral acquisition was less than 5×10^{-9} Torr. Spectra used to determine surface elemental compositions were acquired at an analyzer pass energy of 150 eV. The high-resolution C1s

spectra were acquired at an analyzer pass energy of 50 eV. The take-off angle (the angle between the sample normal and the axis of the analyzer lens) was 55° for all XPS experiments. This take-off angle corresponds to a sampling depth of approximately 5 nm. At least two spots on one or more replicates were analyzed for each sample type.

The Service Physics ESCAVB Graphics Viewer program was used to determine peak areas and calculate elemental compositions. Concentrations of all elements except Al, V and S were determined from 0 – 1000 eV survey scans. Al, V and S concentrations were calculated from 20 eV scans centered around the peaks for those elements. The binding energy scale was calibrated by assigning the hydrocarbon peak in C1s high-resolution spectra to a binding energy of 285.0 eV. Peak fitting of high-resolution C1s spectra employed a Gaussian line shape and was performed using CasaXPS 2.3.11 software.

Time-of-flight Secondary Ion Mass Spectrometry (ToF-SIMS)—ToF-SIMS data was acquired on an ION-TOF TOF.SIMS 5–100 instrument using a pulsed 25 keV, 0.8 pA Bi^+ primary ion source operated in the high current bunched mode and scanned over 150 μm × 150 μm area. Five positive secondary ion and five negative secondary spectra were acquired for each sample type over a mass range from m/z = 0 to 850. The primary ion dose for each spectrum was below the static SIMS limit of 1×10^{12} ions/cm^2. A low-energy electron beam was used for charge compensation. The mass resolution (m/Δm) for positive spectra was typically 5000 for the m/z 27 ($C_2H_3^+$) peak and 11000 for the m/z 25 (C_2H^-) peak in negative spectra. Positive ion spectra were mass calibrated using the CH_3^+, $C_3H_7^+$ and $C_7H_7^+$ peaks and negative ion spectra were mass calibrated using the CH_2^-, C_3^- and C_4H^- peaks. Mass calibration errors were less than 10 ppm. ToF-SIMS peak intensities were normalized to total counts before plotting.

Atomic Force Microscopy (AFM)—Topographic imaging of the substrates before and after polymer grafting was performed with a Molecular Imaging PicoScan (Agilent Technologies, Santa Clara, CA) instrument using contact mode and NP-S tips (Veeco, Santa Barbara, CA) at a scan rate of 3.3 Hz. Two images per sample were acquired from 41 μm × 41 μm areas and flattened by 1st order line flattening.

In vitro studies

Cell culture—MG63 osteoblast-like cells were obtained from the American Type Culture Collection (ATCC) and cultured in Dubelcco's Modified Medium (DMEM) supplemented with 10% fetal calf serum (FCS), 100 U/mL penicillin and streptomycin, and 1% L-glutamine, all from Invitrogen. Cells were plated in a 75 cm^2 flask with 20 mL of culture medium. They were maintained in a humidified 5% CO_2 balanced-air incubator at 37°C until confluence was reached. The medium was changed twice a week. Cells were detached using 10 mL of preheated trypsin-EDTA (Invitrogen) at 37°C for 4 min. The cells were centrifuged and resuspended in culture medium at the desired concentration.

Cell adhesion strength—Ti_{alloy}, Ti_{NaSS} and $Ti_{MA/NaSS}$ disks were placed on the bottom of a 24-well culture plate. 1.2×10^5 MG63cells per well were seeded on the samples for 30 min. After removing the suspension containing non adherent cells, disks were split into 2 groups. In the first group: adhering cells were detached by trypsin digestion to determine N1, the number of adhering cells present before the shear stress was applied. In the second group: adhering cells were exposed to 8 dyn cm^{-2} shear stress for 15 min, according to the procedure described previously (22). Then, still adhering cells after the application of the shear stress were detached by trypsin digestion to determine N2, the number of adherent cells present after the shear stress was applied.

To define the variation of cell adhesion on the different samples, equation (1) was used:

$$\frac{N1-N2}{Nsc} \quad (1)$$

where Nsc is the number of cells initially seeded onto the sample.

Statistical analysis of in vitro experiments—The *in vitro* biological data were analyzed using the Students t-test and one-way ANOVA tables with Fisher's or Tuckey's multiple comparison tests to evaluate statistically significant differences between sample groups. Tuckey's test was used, instead of Fisher's, to compare sample groups with different sample sizes. In both cases, the differences were considered to be significant when $p < 0.05$. All statistical analyses were performed with the MinitabTM software (Minitab release 13.0).

In vivo study

Implantation method—The *in vivo* study was conducted in accordance with the European and French Guidelines for Care and Use of Laboratory Animals (Directive du conseil 24.11.1986, 86/609/CEE), on animal experimentation. Nine adult male rabbits from New Zealand (Segav, Saint-Mars d'Egrenne, France), each weighting 3.5 kg, were used in this study. Animals were housed in individual cages in an environment of 21°C and 50% air humidity and were given water and food ad libitum.

General anaesthesia was induced by intra-muscular injection of 0.5 mg/kg Diazepan (Valium®; Roche; Basel, Switzerland), 0.25 mg/kg metedomidine hydrochloride (Domitor®, Virbac; France), and 100 mg/kg Ketamine hydrochloride (Ketalar 500®, Pfizer; France). The implantation site of the animals was then shaved and disinfected.

Bone defects in the femur condyles were prepared as following: the distal lateral aspect of each femoral condyle was exposed and a cylindrical cavity (6-mm deep and 5.5-mm wide) was created in the lateral condyle in a stepwise fashion under continuous saline irrigation. Eighteen defects were assigned randomly to either grafted alloy titanium samples or to control samples (Ti_{alloy}). Six implants for each of the three surfaces tested (Ti_{alloy}, Ti_{NaSS} and $Ti_{MA/NaSS}$) were randomly placed in the defects. Then the wound was closed in three sequential layers (ligaments, soft tissue, and skin). Analgesics (0.2 mg/kg metoxicamn) (Metakam® Boehringer Ingelheim Vetmedica GmbH Germany) were prescribed in the immediate postoperative period. Antibiotic therapy consisting of sulfadimethoxine trimethoprime (Copylap® Biové; France) at 25 mg/kg, was also administrated each day for 5 days after surgery. In the postoperative period the animals were checked daily. The rabbits were euthanized at 4 weeks postsurgery implantation, using an overdose of pentobarbital. The femoral condyles were excised and cleaned of soft tissue and prepared for histological and histomorphometric analysis.

Histology and histomorphometry—After harvesting, the specimens were fixed in 10% phosphate-buffered formalin solution for 15 days, rinsed in water, dehydrated with ethanol, cleaned in xylene, and embedded in poly (methyl methacrylate). Blocks were sectioned perpendicular to the long axis of each implant to obtain three sections per sample. Each cylinder section was then grounded down to a thickness of 60 μm, using an Exact Grinding System (Exact Aparatebau GmbH Norderstedt, Germany). Then, the surfaces of the sections were stained with Stevenels' blue and van Gieson picro-fuschin for subsequent standard light microscopy and/or histomorphometric analysis.

Three sections per specimen were histomorphometrically analyzed and the peri implant mineralised tissue fraction was measured using custom-made software in conjunction with

an image processing system consisting of a microscope (DBMR Leica, Leica GmbH, Germany) and a video-camera to (CUE-2 Olympus Q1A0150). Once the image was digitized, a circle was drawn at the implant perimeter (yellow line in Figure 1), and another one at a distance of 50 μm around the implant (blue line in Figure 1). Then the area occupied by mineralised tissue was drawn and the percentage was calculated.

Statistical Analysis of in vitro experiments—Numerical data were reported as the mean ± standard deviation (SD). Statistical significance was determined by one-way analysis of variance (ANOVA) and Fisher's PLSD test using Statview 5.0 statistics software (SAS Institute, Berkeley, California). Significance was defined as having a p value < 0.05.

Results and Discussion

Polymer Grafting

Monomers bearing anionic groups were covalently attached to the titanium surface by radical polymerization. Immersion of titanium samples in a mixture of pure sulphuric acid and hydrogen peroxide (30%) produces a surface layer of titanium hydroxide and titanium peroxide species. The existence of the Ti-peroxide radical was proposed by different research groups [30] and [31] based on the presence of bands in the range of 890–900 cm^{-1} in the IR spectra of H_2O_2-oxidized Ti powder. Takemoto et al. have shown that the amount of Ti peroxide present decreases upon heating [31]. Immersion of the titanium samples in a heated aqueous solution of the monomers (NaSS or mixture of MA and NaSS) induces decomposition of the Ti-peroxide radicals and initiates polymerization of the monomers as shown previously on pure titanium (22).

Toluidin Blue—The amount of polyNaSS grafted onto the Ti alloy surfaces, as determined by the Toluidin blue colorimetric method, was 4.2 ± 0.3 μg/cm^2. This value is comparable to the value of 5.0 ± 0.3 μg/cm^2 reported for polyNaSS grafted onto a pure titanium surface (22). Since the toluidine blue method can not distinguish between sulfonate and carboxylate groups (it binds to both), a composition of 80/20 MA/NaSS was assumed for the grafted copolymer film. With this assumption the amount of grafted copolymer measured by Toluidin blue was 1.3 ± 0.3 μg/cm^2. Although by weight this amount is about 3x lower than the amount of grafted polyNaSS, the molecular mass of the NaSS is 2.4x larger than MA (206 vs 86). Thus, on a molar basis the number of monomers present in the two grafted films was similar. Lee et al have observed on polypropylene that the amounts of grafted MA are higher than the amount of grafted polyNaSS (32). Polypropylene is hydrophobic whereas the oxidized titanium surface is hydrophilic. (The water contact angle on the oxidized Ti alloy surface was 32° ± 2°). NaSS is more strongly ionized than MA, which should make it easier for NaSS to approach and react with the hydrophilic Ti surface. This could explain why the different grafting behavior of NaSS and MA on oxidized Ti and polyproplyene surfaces is observed.

The Toluidine blue assay did not detected any significant difference between the amounts of grafted polyNaSS or copolymer on Ti alloy surfaces oxidized for 1 or 3 min. However, it was able to show significant amounts of polyNaSS and the copolymer were grafted onto the oxidized titanium alloy surfaces.

Surface Characterization

XPS—The XPS determined surface elemental compositions for oxidized Ti6Al4V before and after grafting with NaSS or MA/NaSS are summarized in Table 1. The theoretical values expected for Ti6Al4V, NaSS and MA/NaSS based on their stoichiometry are also shown in Table 1 for comparison.

Within experimental error, the carbon, oxygen, titanium and sulfur concentrations of the Ti6Al4V samples oxidized for 1 and 3 min are the same. The oxygen detected on these samples is consistent with formation of an oxide/peroxide/hydroxide overlayer formed by the oxidation treatment. The presence of carbon is likely due to adventitious hydrocarbon deposition onto the sample surfaces since these samples were exposed to air prior to the XPS analysis. The small amount of sulfur detected on these surfaces probably is from the use of sulfuric acid in the oxidation process. Small amounts of alumimun (2–3 atomic percent) and trace amounts of vanadium (0.2 to 0.3 atomic percent) were detected on the oxidized Ti6Al4V surfaces. The only difference between the two oxidized Ti6Al4V surfaces was that sodium was detected on the sample oxidized for 3 min. Additionally, calcium (ca. 1 atomic percent) was detected on both oxidized samples while phosphorus (ca. 3 atomic percent) and trace amounts of zinc were detected only on the sample oxidized for 3 min.

After grafting the 1 and 3 min oxidized samples with NaSS significant decreases in titanium and oxygen concentrations along with significant increases in sulfur and carbon concentrations were observed, consistent with changes expected for NaSS grafting onto the surface of oxidized Ti6Al4V. The concentration changes were slightly larger for the sample oxidized for 3 min, indicating slightly more NaSS was grafted onto this surface. After grafting MA/NaSS onto the 1 min oxidized sample the concentration changes were similar, except for sulfur, to those observed for polyNaSS grafted onto the same surface, indicating similar levels of grafting for the NaSS and MA/NaSS onto 1 min oxidized Ti6Al4V surfaces. This is consistent with the Toluidin blue results that show similar grafting of polyNasSS and the copolymer on a molar basis. The lower NaSS concentration in the MA/NaSS copolymer is probably the reason a lower sulfur concentration is detected by XPS on the MA/NaSS grafted surface. Only small changes in the carbon, oxygen and titanium concentrations were observed after the MA/NaSS grafting reaction on the Ti6Al4V oxidized for 3 min, indicating little copolymer grafting occurred on this surface. It is not clear why significantly less grafted MA/NaSS was detected on the 3 min oxidized sample, but possibly the MA/NaSS mixture is more sensitive to the higher levels of contaminants (sodium, phosphorous and zinc) detected on this sample. Also, the 3 min oxidized sample is significantly rougher than the 1 min oxidized sample (see AFM results below; Figure 3; Table 3).

For all grafted samples the decrease in oxygen and titanium concentrations is consistent with attenuation of XPS oxygen and titanium signals from the oxidized Ti6Al4V substrate by the grafted polymer overlayer. Likewise, the increase in the XPS carbon and sulfur signals in the grafted samples is due to the presence of grafted polymer overlayer. For all grafted polymer surfaces the Na/S was significantly below the expected value of 1 from the NaSS structure. This is in contrast to previous results for NaSS grafting on poly(ethylene terephthalate) [27, 29] and indicates the Na was removed during the final rinsing of the samples.

The XPS high-resolution C1s spectra of the oxidized Ti6Al4V surface before and after grafting with NaSS and MA/NaSS are shown in Figure 2. The spectral area under each curve has been normalized to total carbon atomic concentration observed for that sample. Note from Table 1 the carbon atomic percent is 1.6 to 1.8 times higher on the 3 samples where significant grafting has occurred (NaSS on 1 and 3 min oxidized Ti6Al4V; MA/NaSS on 1 min oxidized Ti6Al4V) compared to the starting oxidized surfaces. The peak fitting results from these spectra are listed in Table 2 show the percentage of species present in the total carbon spectrum for each sample. The expected amounts of each carbon species based on the stoichiometry of NaSS and MA/NaSS are also listed in Table 2. Note that the adventitious carbon present on the oxidized Ti6Al4V surfaces contains at least three types of carbon species, a hydrocarbon species near 285 eV, a C-O species near 286.5 eV and a

carboxylic species near 289 eV. These overlap with the species expected from NaSS (hydrocarbon and C-SO_3) and MA (hydrocarbon and carboxylic acid). For grafting onto the 1 min oxidized surfaces the percent of hydrocarbon species increased slightly while the percent of carboxylic species decreased slightly. More importantly the ratio of hydrocarbon to carboxylic species was higher on the NaSS grafted surface compared to the MA/NaSS graft surface, as expected since that ratio is higher in NaSS compared to MA. The highest hydrocarbon percentage and lowest carboxylic species percentage were observed from the sample where NaSS was grafted onto the 3 min oxidized Ti6Al4V surface. A small shakeup satellite from the aromatic ring in NaSS was also detected on this sample. These observations are consistent with the fact that the XPS determined surface elemental compositions indicated NaSS grafting on the 3 min oxidized Ti6Al4V surface produced a slightly thicker polymer overlayer. The distribution of carbon species observed from grafting MA/NaSS onto the 3 min oxidized Ti6Al4V surface was not noticeably different from the starting oxide surface, consistent with the observed surface elemental composition of this sample.

AFM—The AFM determined average surface roughness of the oxidized Ti6Al4V surfaces before and after polymer grafting are listed in Table 3. Representative images of the two oxidized surfaces before grafting are shown in Figure 3. As shown in Table 3, increasing the oxidation treatment time from 1 to 3 min resulted in a doubling of the surface roughness.

ToF-SIMS—All three species of interest for this investigation, titanium oxide, NaSS and MA, have characteristic peaks in the negative secondary ion spectra, so the ToF-SIMS results will focus on that data. The intensity of the peak at m/z = 97.94, which can be assigned to $TiO_3H_2^-$, correlated well with the XPS measured titanium concentrations (see Figure 4a), indicating the intensity of this ToF-SIMS peak is related to the grafted polymer thickness. The highest $TiO_3H_2^-$ intensity corresponded to samples with no grafted films, while the lowest $TiO_3H_2^-$ intensity corresponded to the sample with the thickest grafted film (NaSS on 3 min oxidized Ti6Al4V). Note when the ToF-SIMS $TiO_3H_2^-$ signal is expolated to zero that would correspond to an XPS composition of 5–6 atomic percent titanium. This is because the XPS sampling depth (ca. 5 nm) is significantly larger than the ToF-SIMS sampling depth (ca. 2 nm) allowing XPS to detect signals from the titanium substrate when the overlayer is thicker than the ToF-SIMS sampling depth but thinner than the XPS sampling depth.

As sulfur is an atom that is unique to NaSS, there are several sulfur containing peaks in the negative secondary ion spectra that can be used to characterize the NaSS content of the grafted film. Both S^- and SO^- (fragments of the sulfonate group) correlated linearly with atomic percent sulfur measured by XPS (see Figures 4b and 4c). Thus, the intensity of these peaks can be used to measure the relative concentration of NaSS in the grafted films. For example, based on the attenuation of the XPS and ToF-SIMS titanium signals, the NaSS and MA/NaSS grafted films on the 1 min oxidized Ti6Al4V substrates have similar thicknesses, while based on the XPS and ToF-SIMS sulfur signals the MA/NaSS copolymer film, as expected, has a lower NaSS content. Fragments corresponding to the benzene ring with sulfonate group ($C_6H_4SO_3^-$) and the NaSS monomer unit minus sodium ($C_8H_7SO_3^-$) at m/z = 155.98 and 183.00, respectively, were detected from all grafted surfaces. However, unlike the intensities of the S^- and SO^- peaks, the intensities of these molecular fragments did not correlate linearly with the NaSS surface concentration (see Figure 5). This indicates the intensity of these fragments is strongly influenced by matrix effects, (i.e., the concentration of other species in the sample). For grafted films of different thickness (e.g., NaSS grafted onto 1 and 3 min oxidized Ti6Al4V) it appears the $C_6H_4SO_3^-$ and $C_8H_7SO_3^-$ intensities in the thinner grafted film are enhanced by the titanium oxide surface. For grafted films of similar thickness (e.g., NaSS and the copolymer on 1 min oxidized Ti6Al4V) it appears that

the $C_6H_4SO_3^-$ and $C_8H_7SO_3^-$ intensities in the mixed grafted film are enhanced by the presence of the MA groups. Apparently the presence of the titanium oxide and MA species increase the probability that negatively charged NaSS molecular fragments will be formed and ejected during the ToF-SIMS experiment.

The characteristic peak from MA is at m/z = 85.03. This peak corresponds to the MA monomer unit minus a hydrogen ($C_4H_5O_2^-$) and is observed in the negative ion spectra of all methacrylate polymers (34 – 36). As shown in Figure 6 the intensity of this peak is highest for the two grafted MA/NaSS films and nearly zero for the two grafted NaSS films. Note that the ungrafted oxidized Ti6Al4V surface has a $C_4H_5O_2^-$ peak intensity that falls between the grafted MA/NaSS and grafted NaSS surfaces. This is consistent with the XPS C1s spectrum from oxidized Ti6Al4V, which shows the adventitious carbon species on this surface have similar chemistries (e.g., carboxylic species) to MA.

Biological Studies

Cell adhesion strength—From Equation (1) defined in Materials and Method, it was possible to compare the results of cell adhesion from each grafted surface to the non grafted control surface. The results are reported in Figure 7.

As can be seen from the form of equation (1) the lower the value of (N1 – N2)/Ncs, the fewer the number of cells that are detached by application of the shear stress (i.e., N1 – N2 goes to zero as no cells are detached by the shear stress). The comparison of the ratios for the different samples shows that after application of 8 dyn/cm^2 shear force a higher percentage of cells are detached from Ti_{NaSS} compared to $Ti_{MA/NaSS}$. The percent of cells detached by shear force from the ungrafted surface, Ti_{alloy}, fell between those of the grafted surfaces. Thus, the grafting of sulfonate groups onto oxidized Ti6AL4V appears to favour the adhesion of cells that are capable of resisting detachment under a shear force of 8 dyn/cm^2. This is consistent with previous results reported with MG63 cells cultured on pure titanium (22). For $Ti_{MA/NaSS}$, the value of Equation (1) is 65% higher than that measured for Ti_{alloy} which means that the presence of sulfonate and carboxylic groups allows more MG63 cells to detach under a shear force of dyn/cm^2. This result is surprising because we have shown that the synergic effect of both groups grafted on pure titanium is quite favourable to cellular adhesion (unpublished results). However in the case of pure titanium, the cell attachment was almost identical for titanium surfaces grafted with polyNaSS or poly(NaSS-MA), regardless of the chemical composition of the grafted polymer. Thus further studies of the influence of the grafted copolymer chemical composition on the cell adhesion and detachment processes are needed.

In vivo assessment—The performance of grafted alloy titanium implants was evaluated *in vivo* in femoral rabbit model by histology and quantitative histomorphometry. All rabbits were ambulatory within 3 hours after surgery. No infection was observed during this study. After four weeks post-implantation, bone was in direct contact with the surfaces of all implants tested (see Figure 8). No fibrous encapsulation of the implants was observed in any histological sections. Both control and grafted implants were surrounded by lamellar trabecular bone with wide haversian canals lined by osteoblasts. The non-mineralized tissue was composed of bone marrow, matrix components, vascular structures and cells. At 4 weeks post-implantation, the percent of mineralised tissue fraction for Ti_{NaSS} and Ti_{alloy} implants were similar (59% ± 4% and 57% ± 5%, respectively) and higher ($p<0.05$) than for $Ti_{MA/NaSS}$ (47 ± 5%), as shown in Figure 9.

Thus while grafted polyNaSS does not affect the mineralized content in the tissue surrounding the implant, the grafted MA/NaSS copolymer does slightly decrease the mineralized content in the surrounding tissue. These preliminary results indicate that Ti_{NaSS}

is osteointegrable and of clinical interest. Further studies of the long-term bone response to the Ti_{NaSS} surfaces are needed. To our knowledge, no results have been previously published on bone response around titanium or Ti6Al4V surfaces grafted with sulfonate and carboxylate groups.

Conclusions

NaSS and MA/NaSS coatings were successfully grafted onto the surface of oxidized Ti6Al4V alloy implants. The the grafted polymers were characterized by Toluidin Blue, XPS, ToF-SIMS and AFM. The piranha oxidization treatment significantly roughened the Ti alloy surface, especially when the samples were treated for 3 min (AFM measured surface roughness increased 2x when the treatment time was increased from 1 to 3 min). Based on the AFM observations, coupled with the XPS and ToF-SIMS results that showed higher levels of unexpected elements (Na, P, Ca, Zn, etc.) indicate a 3 minute piranha treatment is too severe for Ti6Al4V samples and it is recommended that future oxidation treatments be done for shorter times and use lower concentration piranha solutions. Further evidence for this recommendation is the variability observed in the grafting efficiency of the MA/NaSS coatings on the Ti alloy samples oxidized for 3 min (Toluidin Blue detected significant grafting while XPS and ToF-SIMS did not). Toluidin Blue, XPS and ToF-SIMS all showed significant amounts of NaSS and MA/NaSS were grafted onto the Ti alloy surfaces oxidized for 1 minute. Preliminary *in vivo* studies using the femoral rabbit model seem to showed promising results for the grafted implants (remark of reviewer 6). After 4 weeks of implantation bone was observed to be in direct contact with the surface of the implants and significant amounts of mineralized tissue was found to be present adjacent to the implant surfaces. Also, no infection was observed in these 4-week implant surfaces.

Acknowledgments

The XPS, ToF-SIMS and AFM experiments were done at the National ESCA and Surface Analysis Center for Biomedical Problems, which is funded by the US National Institutes of Health through grant EB-002027. Dr. James Hull is thanked for providing the AFM results.

Reference List

1. Ratner BD, Hoffman AS, Shoen FJ, Lemons JE. Biomaterials Science; An Introduction to Materials in Medicine. Part I Materials Science and Engineering (2). 2:138–152.Part II Biology, Biochemistry and Medicine. 7:527–555.
2. Breme J. Titanium and titanium alloys, biomaterials of preference. Revue de Metallurgie. 1989; 10:625–637.
3. Huber M, Reinisch G, Trettenhahn G, Zweymüller K, Lintner F. Presence of corrosion products and hypersensitivity-associated reactions in periprosthetic tissue after aseptic loosening of total hip replacements with metal bearing surfaces. Acta Biomaterialia. 2009; 5:172–180. [PubMed: 18725188]
4. Long M, Rack HJ. Titanium alloys in total joint replacement-a materials science perspective. Biomaterials. 1998; 19:1621–1639. [PubMed: 9839998]
5. Geetha M, Singh AK, Asokamani R, Gogia AK. Ti based biomaterials, the ultimate choice for orthopaedic implants" - a review. Progress in Materials Science. In Press, Accepted Manuscript.
6. De Groot K, Geesink R, Klein CPAT, Serekian P. Plasma sprayed coatings of hydroxylapatite. Journal of Biomedical Materials Research. 1987; 21(12):1375–1381. [PubMed: 3429472]
7. Ramires PA, Romito A, Cosentino F, Milella E. The influence of titania/hydroxyapatite composite coatings on in vitro osteoblasts behaviour. Biomaterials. 2001; 22(12):1467–1474. [PubMed: 11374445]
8. Deng C, Wang Y, Mang YP, Gao JC. In situ laser coating of calcium phosphate on TC4 surface for enhancing bioactivity. Journal of Iron and Steel Research International. 2007; 14(3):73–78.

9. Xinbo XB, Zou CF, Feng YP, Zeng XR, Xie SH. Exploration of preparation for bioactive calcium phosphate coating by using high frequency induction heat gradient technique of Ti6A14V. Rare Metal Materials and Engineering. 2007; 36(7):1249–1252.
10. Ogiso M, Yamamura M, Kuo PT, Borgese D, Matsumoto T. Comparative push-out test of dense HA implants and HA-coated implants: Findings in a canine study. Journal of Biomedical Materials Research. 1998; 39(3):364–372. [PubMed: 9468044]
11. Ogiso M, Yamashita Y, Matsumoto T. Differences in microstructural characteristics of dense HA and HA coating. Journal of Biomedical Materials Research. 1998; 41(2):296–303. [PubMed: 9638535]
12. Filip P, Kneissl AC, Mazanec K. Physics of hydroxyapatite plasma coatings on TiNi shape memory materials. Materials Science and Engineering A-Structural Materials Properties Microstructure and Processing. 1997; 234:422–425.
13. Kokubo T. Design of bioactive bone substitutes based on biomineralization process. Materials Science & Engineering C-Biomimetic and Supramolecular Systems. 2005; 25(2):97–104.
14. Wen HB, de Wijn JR, Cui FZ, de Groot K. Preparation of bioactive Ti6Al4V surfaces by a simple method. Biomaterials. 1998; 19(1–3):215–221. [PubMed: 9678870]
15. De Maeztu MA, Alava JI, Gay-Escoda C. Ion implantation: surface treatment for improving the bone integration of titanium and Ti6Al(4)V dental implants. Clinical Oral Implants Research. 2003; 14(1):57–62. [PubMed: 12562366]
16. Hao L, Lawrence J. Wettability modification and the subsequent manipulation of protein adsorption on a Ti6Al4V alloy by means of CO2 laser surface treatment. Journal of Materials Science-Materials in Medicine. 2007; 18(5):807–817. [PubMed: 17171456]
17. Lawrence J, Hao L, Chew HR. On the correlation between Nd: YAG laser-induced wettability characteristics modification and osteoblast cell bioactivity on a titanium alloy. Surface & Coatings Technology. 2006; 200(18–19):5581–5589.
18. Saldana L, Barranco V, Gonzalez-Carrasco JL, Rodriguez M, Munuera L, Vilaboa N. Thermal oxidation enhances early interactions between human osteoblasts and alumina blasted Ti6Al4V alloy. Journal of Biomedical Materials Research Part A. 2007; 81A(2):334–346. [PubMed: 17120220]
19. Saldana L, Vilaboa N, Valles G, Gonzalez-Cabrero J, Munuera L. Osteoblast response to thermally oxidized Ti6Al4V alloy. Journal of Biomedical Materials Research Part A. 2005; 73A(1):97–107. [PubMed: 15704115]
20. Liang FH, Lian Z. Research and development on surface bioactivity methods of titanium and its alloys. Rare Metal Materials and Engineering. 2003; 32(4):241–245.
21. Mayingi J, Hélary G, Noirclère F, Bacroix B, Migonney V. Grafting of bioactive polymers onto titanium surfaces and human osteoblasts response. IRBM. 2008; 29:1–6.
22. Hélary G, Noirclère F, Mayingi J, Migonney V. A new approach to graft bioactive polymer on titanium implants: Improvement of MG 63 cell differentiation onto this coating. Acta Biomaterialia. 2009; 5:124–133. [PubMed: 18809363]
23. Dubruel P, Vanderleyden E, Bergada M, De Paepe I, Chen H, Kuypers S, et al. Comparative study of silanisation reactions for the biofunctionalisation of Ti-surfaces. Surface Science. 2006; 600(12):2562–2571.
24. Viornery C, Chevolot Y, Leonard D, Aronsson BO, Pechy P, Mathieu HJ, et al. Surface modification of titanium with phosphonic acid to improve bone bonding: Characterization by XPS and ToF-SIMS. Langmuir. 2002; 18(7):2582–2589.
25. Viornery C, Guenther HL, Aronsson BO, Pechy P, Descouts P, Gratzel M. Osteoblast culture on polished titanium disks modified with phosphonic acids. Journal of Biomedical Materials Research. 2002; 62(1):149–155. [PubMed: 12124796]
26. Yammine P, Pavon-Djavid G, Hélary G, Migonney V. Surface modification of silicone intraocular implants to inhibit cell proliferation. Biomacromolecules. 2005; 6 (5):2630–2637. [PubMed: 16153101]
27. Pavon-Djavid G, Gamble LJ, Ciobanu M, Gueguen V, Castner DG, Migonney V. Bioactive Poly(ethylene terephthalate) Fibers and Fabrics: Grafting, Chemical Characterization, and Biological Assessment. Biomacromolecules. 2007; 8:3317–3325. [PubMed: 17929865]

28. Sano S, Kato K, Ikada Y. Introduction of functional groups onto the surface of polyethylene for protein immobilization. Biomaterials. 1993; 14:817–822. [PubMed: 8218735]

29. Ciobanu M, Siove A, Gueguen V, Gamble LJ, Castner DG, Migonney V. Radical Graft Polymerization of Styrene Sulfonate on Poly(ethylene terephthalate) Films for ACL Applications: "Grafting From" and Chemical Characterization Biomacromolecules. 2006; 7:755–760.

30. Tengvall P, lundstrom I, Sjoqvist, Elwing H, Bjursten LM. Titanium-hydrogen peroxide interaction: model studies of the influence of the inflammatory response on titanium implants. Biomaterials. 1989; 10(3):166–175. [PubMed: 2541819]

31. Takemoto S, Yamamoto T, Tsuru K, Hayakawa S, Osaka A, Takashima S. Platelet adhesion on titanium oxide gels: effect of surface oxidation. Biomaterials. 2004; 25(17):3485–3492. [PubMed: 15020122]

32. Lee SW, bondar Y, Han DH. Synthesis of polypropylene fabric with sulfonate Group. Radiation physics and chemistry. 2008; 77(4):503–510.

33. Chilkoti A, Castner DG, Ratner BD. Static Secondary Ion Mass Spectrometry and X-Ray Photoelectron Spectroscopy of Deuterium- and Methyl-Substituted Polystyrene. Applied Spectroscopy. 1991; 45:209–217.

34. Briggs D. Analysis of polymer surfaces by SIMS. 2 - fingerprint spectra from simple polymer films. Surface and Interface Analysis. 1982; 4:151–155.

35. Hearn MJ, Briggs D. Analysis of polymer surfaces by SIMS. 12. On the fragmentation of acrylic and methacrylic homopolymers and the interpretation of their positive and negative ion spectra. Surface and Interface Analysis. 1988; 11:198–213.

36. Davies MC, Lynn RAP, Hearn J, Paul AJ, Vickerman JC, Watts JF. Surface Chemical Characterization Using XPS and ToF-SIMS of Latex Particles Prepared by the Emulsion Copolymerization of Methacrylic Acid and Styrene. Langmuir. 1996; 12:3866–3875.

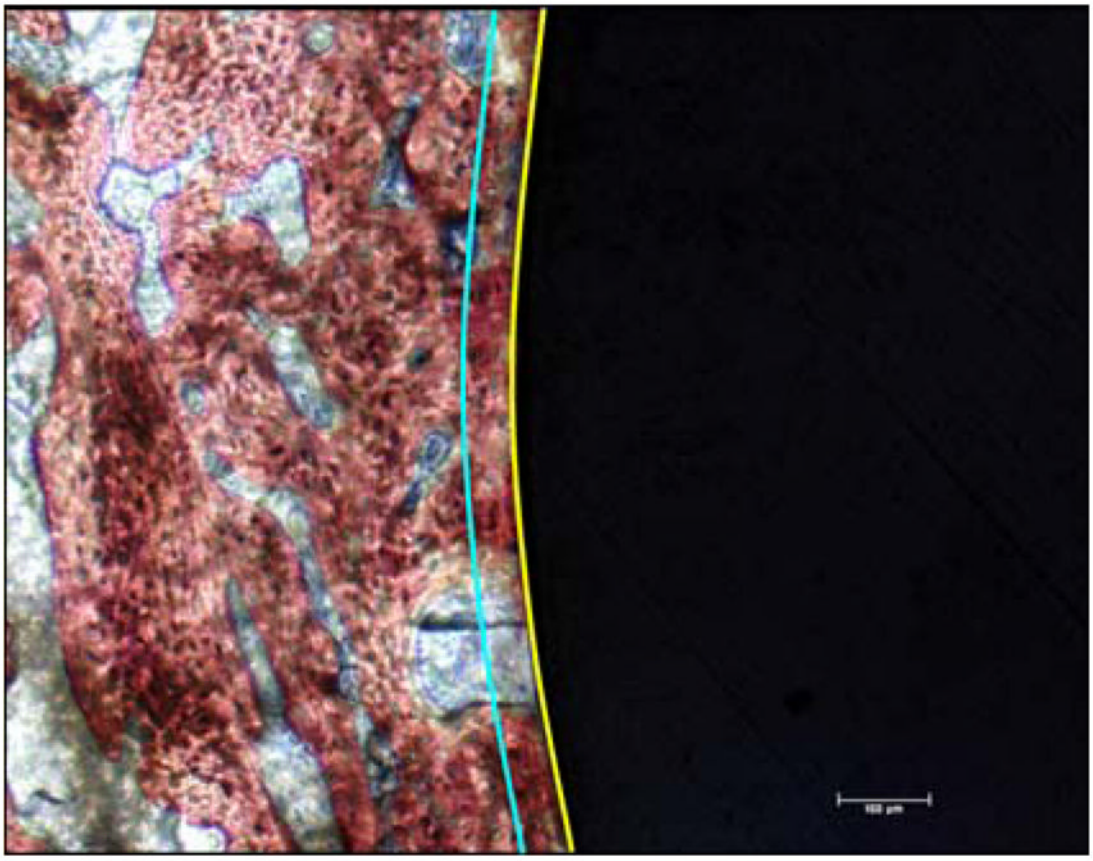

Figure 1.
Example of specimen section used to calculate the percentage of mineralized area surrounding the implant. The black region corresponds to the implant, the yellow line represents the implant perimeter and the blue line represents a distance 50 μm away from the implant perimeter.

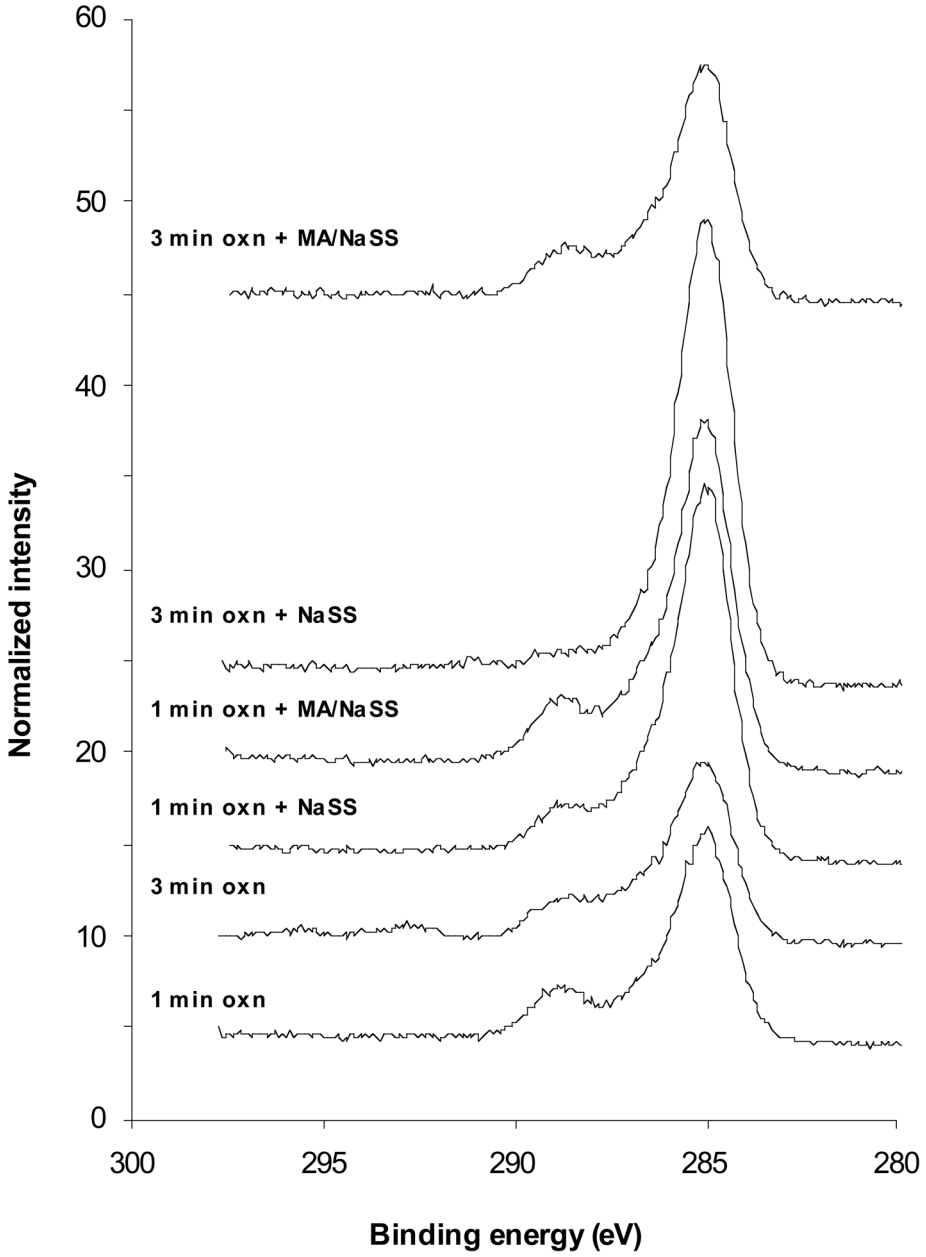

Figure 2.
High resolution C1s spectra of the oxidized Ti6Al4V surface before and after grafting with NaSS or MA/NaSS.

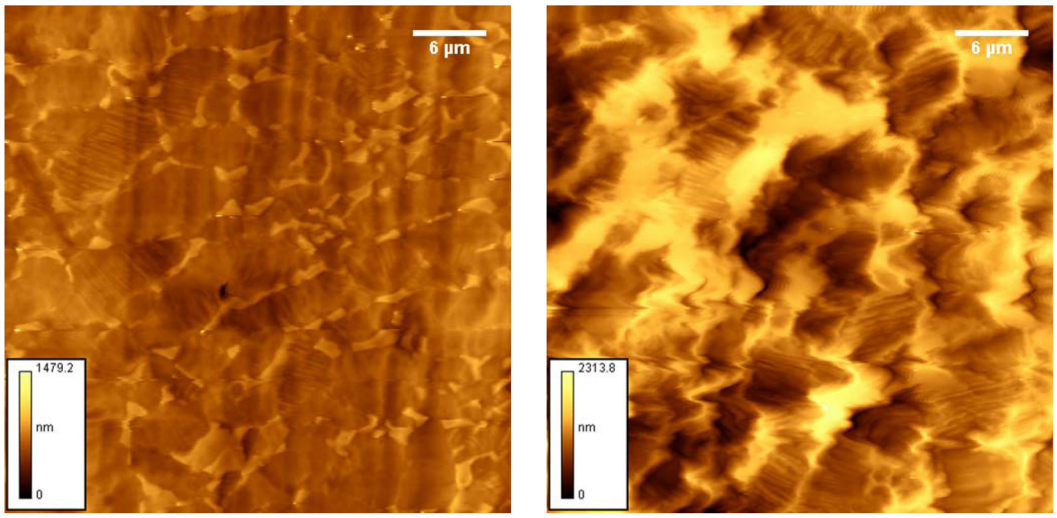

(a) (b)

Figure 3.
41 µm × 41 µm AFM images of Ti6Al4V oxidized for (a) 1 min and (b) 3 min. Scale bars in the lower left corner of each image indicate the maximum peak height R_p.

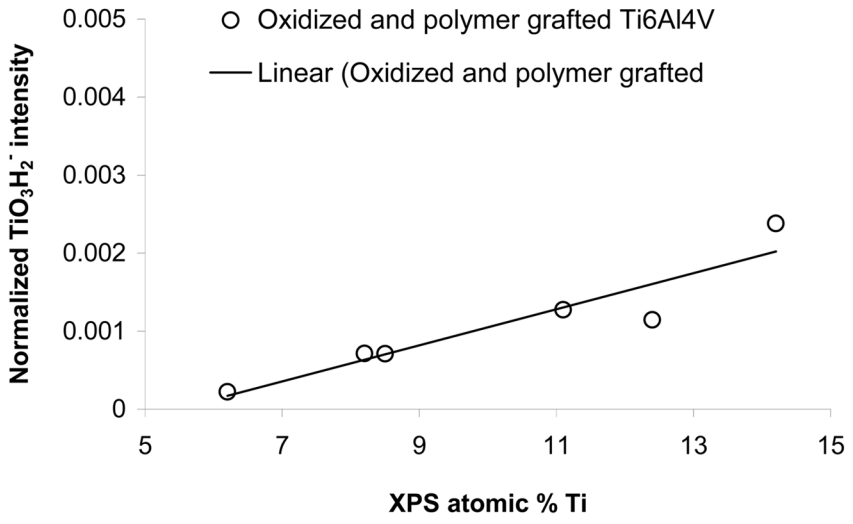

(a)

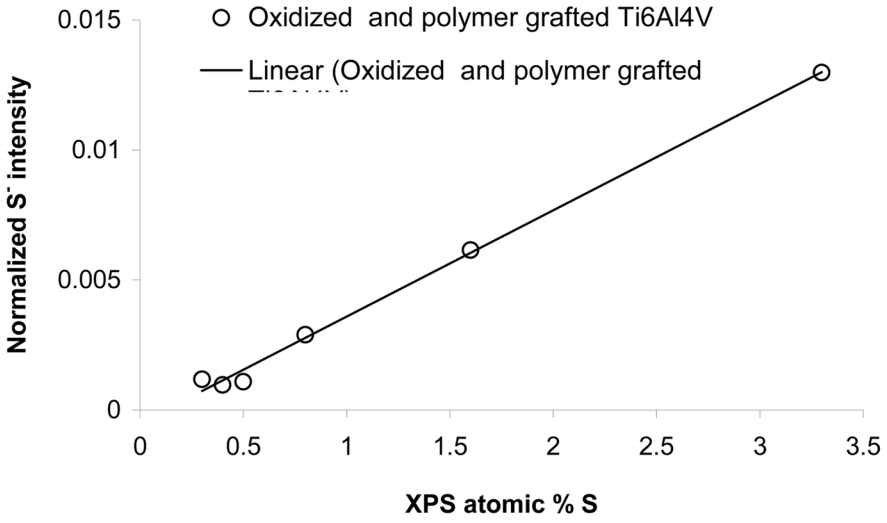

(b)

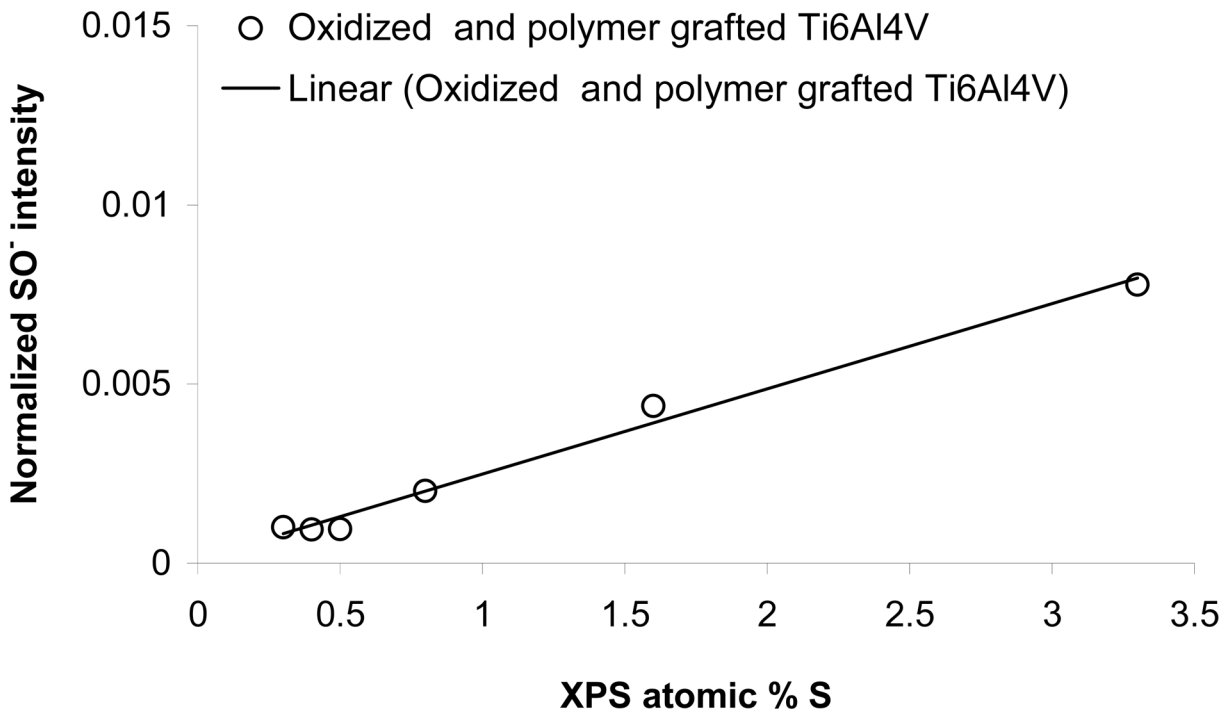

(c)

Figure 4.
ToF-SIMS peak intensities versus XPS atomic percents for (a) $TiO_3H_2^-$ versus % Ti (b) S^- versus % S and (c) SO^- versus % S.

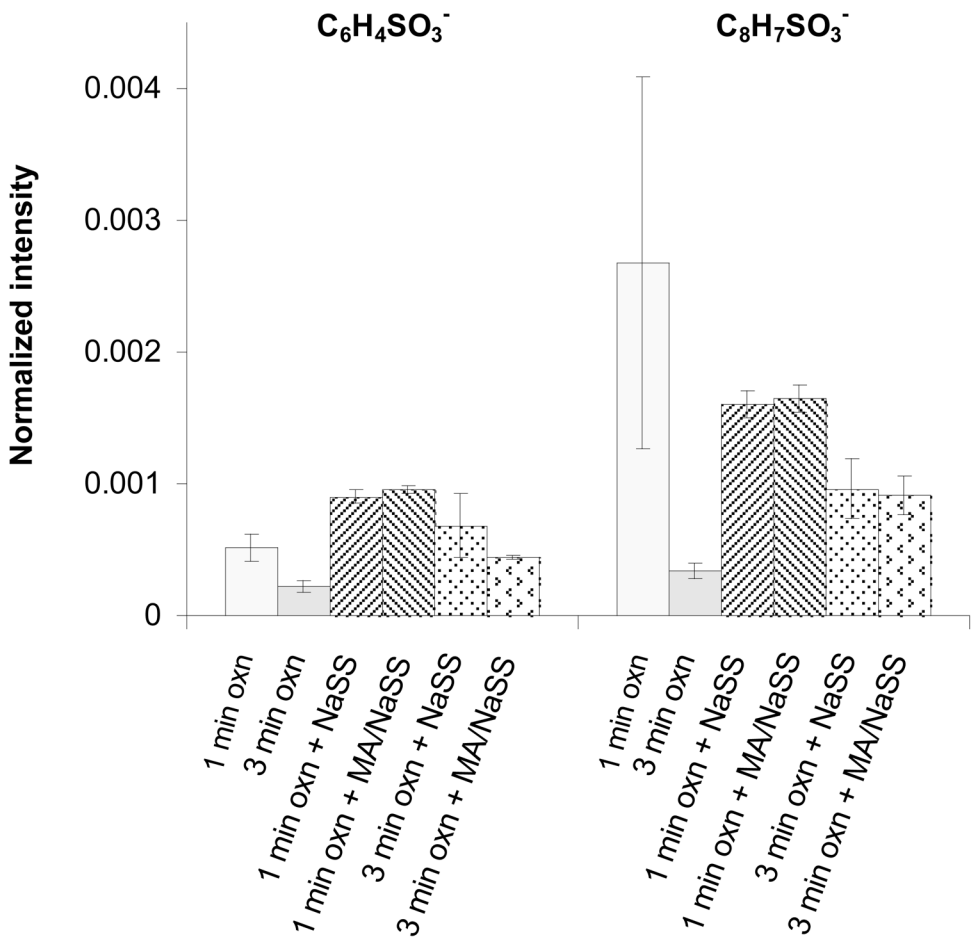

Figure 5.
ToF-SIMS intensities from the benzyl sulfonate group ($C_6H_4SO_3^-$) and the NaSS monomer unit minus sodium ($C_8H_7SO_3^-$) for oxidized Ti6Al4V before and after polymer/copolymer grafting.

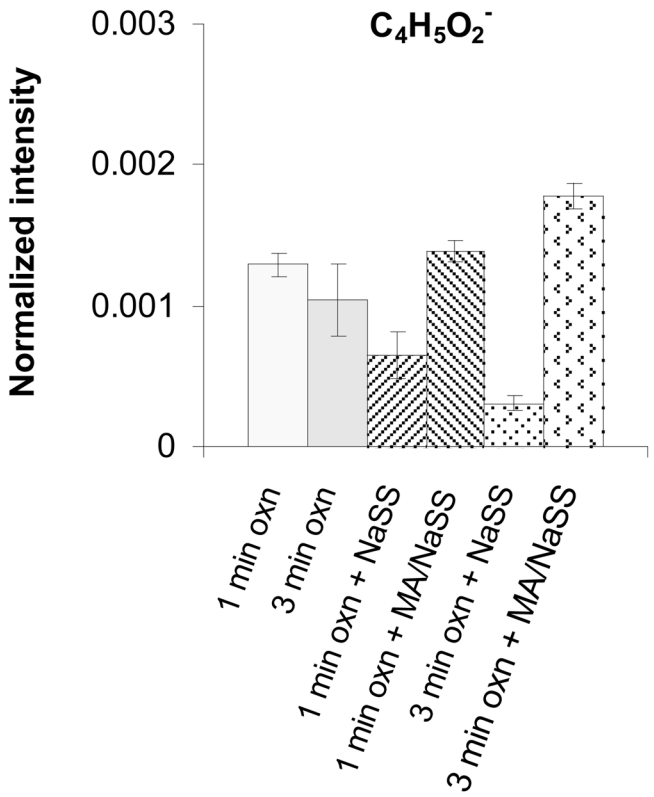

Figure 6.
ToF-SIMS intensities from the methacrylate monomer unit minus a hydrogen ($C_4H_5O_2^-$) for oxidized Ti6Al4V before and after polymer/copolymer grafting.

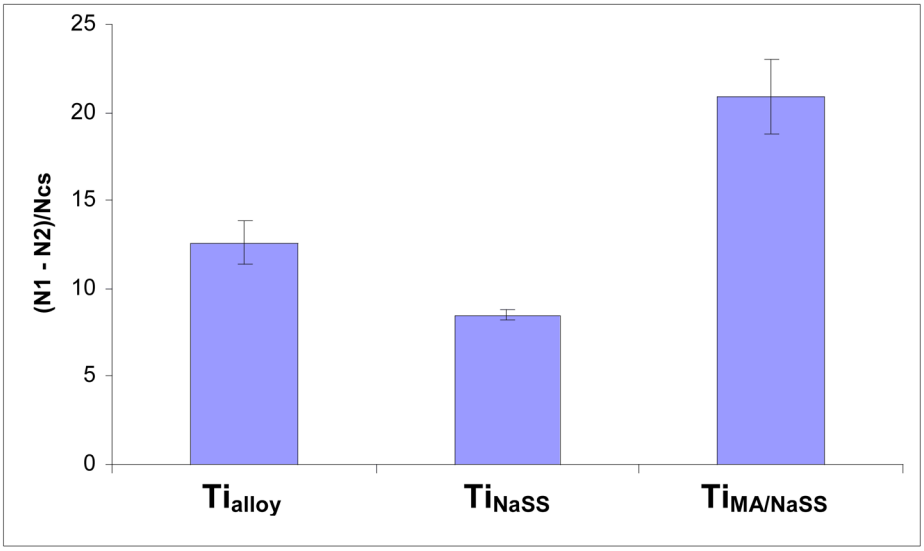

Figure 7.
MG63 cell adhesion results for ungrafted (Ti_{alloy}), NaSS grafted (Ti_{NaSS}) and MA/NaSS grafted ($Ti_{MA/NaSS}$) surfaces compared using Equation (1).

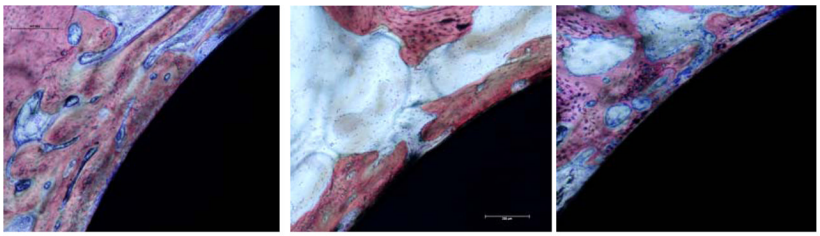

Figure 8.

Micrographs (A: Ti_{alloy}, B: Ti_{NaSS} and C: $Ti_{MA/NaSS}$) of representative histology sections after 4 weeks of implantation. Bone tissue (stained pink) was present around all the surfaces of all implants. Stains used included Stevenels' blue for visualization of the cell nuclei and van Gieson picro-fushin for staining the bone tissue.

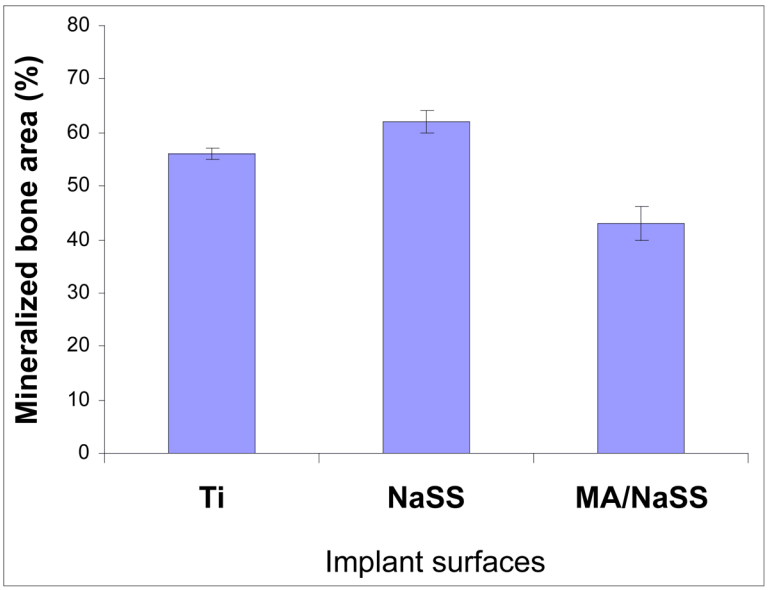

Figure 9.
Percent of mineralized tissue surrounding the implant surfaces (Ti_{alloy}, Ti_{NaSS} and $Ti_{MA/NaSS}$) after 4 weeks of implantation in the femoral rabbit model.

Table 1

XPS determined surface elemental compositions of oxidized Ti6Al4V before and after grafting with NaSS or MA/NaSS.[a]

	XPS Atomic Percent					
Sample type	**Carbon**	**Oxygen**	**Titanium**	**Sulfur**	**Sodium**	**Other**
Ti6Al4V (theory)	-	-	86.2	-	-	-
Oxidized (1 min) Ti6Al4V	28.0 ± 2.2	53.5 ± 1.3	14.2 ± 0.9	0.3 ± 0.1	nd	Al, Ca, V
Oxidized (3 min) Ti6Al4V	25.8 + 1.3	53.2 + 0.1	12.4 + 1.3	0.5 + 0.1	1.5 + 0.2	Al, Ca, V, P, Zn
Oxidized (1 min) Ti6Al4V grafted with NaSS	44.4 ± 1.8	40.1 ± 0.8	8.5 ± 0.8	1.6 ± 0.4	nd	Al, Ca, P, N, V
Oxidized (1 min) Ti6Al4V grafted with MA/NaSS	45.0 ± 0.5	42.2 ± 0.6	8.2 ± 0.6	0.8 ± 0.1	nd	Al, Ca, V, Zn
Oxidized (3 min) Ti6Al4V grafted with NaSS	47.2 ± 5.4	36.5 ± 3.2	6.2 ± 1.3	3.3 ± 0.7	0.4 + 0.6	Ca, F, P, Al, N, V
Oxidized (3 min) Ti6Al4V grafted with MA/NaSS	31.3 ± 0.9	48.9 ± 0.7	± 0.4	0.4 ± 0.1	0.4 + 0.3	P, Al, Ca, F, N, V, Zn
NaSS (theory)	61.5	23.1	-	7.7	7.7	-
MA/NaSS (theory)	64.9	29.7	-	2.7	2.7	-

[a]The expected XPS elemental compositions based on the stoichiometry of Ti6Al4V, NaSS and MA/NaSS are included for comparison. Values are reported as averages. Errors represent one standard deviation. The atomic percent of other elements present in each type of sample is listed in decreasing order. nd = not detected.

Table 2

XPS high-resolution C1s peak fitting results for oxidized Ti6Al4V before and after grafting with NaSS or MA/NaSS.[a]

	XPS C1s Percent			
Sample type	**C-C/C-H**	**C-O/C-SO_3**	**O-C=O**	**Shake-up satellite**
Oxidized (1 min) Ti6Al4V	67	16	17	-
Oxidized (3 min) Ti6Al4V	64	20	16	-
Oxidized (1 min) Ti6Al4V grafted with NaSS	72	18	10	-
Oxidized (1 min) Ti6Al4V grafted with MA/NaSS	69	17	14	-
Oxidized (3 min) Ti6Al4V grafted with NaSS	84	11	3	2
Oxidized (3 min) Ti6Al4V grafted with MA/NaSS	66	18	16	-
NaSS (theory) [b]	(81)	(12)	-	7
MA/NaSS (theory) [b]	78	4	16	1

[a] The expected XPS carbon species based on the stoichiometry of NaSS and MA/NaSS are included for comparison.

[b] The shake-up satellite calculation assumes the NaSS shake-up intensity to be the same as that previously published for polystyrene in reference **33.**

Table 3

AFM roughness results for oxidized Ti6Al4V before and after grafting with NaSS or MA/NaSS.

	Roughness (microns)	
Sample type	**1 min oxidized**	**3 min oxidized**
Oxidized Ti6Al4V	0.60 ± 0.03	1.1 ± 0.001
Oxidized Ti6Al4V grafted with NaSS	0.46 ± 0.03	1.4 ± 0.1
Oxidized Ti6Al4V grafted with MA/NaSS	0.62 ± 0.04	1.3 ± 0.2